Frequency effects on fatigue crack growth and crack-tip domain switching behavior in a lead zirconate titanate ceramic

Soodkhet Pojprapai (Imlao), Jennifer Russell, John. E. Daniels, Mark Hoffman

Abstract

The microstructural origins of the effect of frequency on fatigue behavior of pre-cracked soft ferroelectric $Pb(Zr_{0.48}Ti_{0.52})O_3$ is investigated via a high spatial resolution hard x-ray synchrotron source. It is found that there is a strong link between the frequency of the applied bipolar field, domain switching (fatigue) behavior in terms of ferroelastic reorientation of the domains around the crack tip and the resultant crack growth. The crack growth is accentuated under increased ferroelastic switching and, in particular, found to be more pronounced under low frequency loading. The concept of domain wall viscoelasticity is applied to explain why lower frequencies accelerate crack growth under a bipolar electric field.

Introduction

In this work, the degradation of macroscopic polarization reflecting bulk ferroelectric performance was investigated using electrical fatigue testing equipment. Moreover, a state-of-the-art high energy x-ray diffraction technique is employed to explore domain switching behavior of pre-cracked samples enabling a quantitative analysis of domain texture around the crack tip under a bipolar cyclic electrical load at various frequencies. The concept of viscosity and domain wall movement is employed to explain the micromechanism of domain-switching-induced crack growth under various loading frequencies.

Experimental procedure

Three samples obtained from the same production lot of the bulk samples were cut into a rectangular shape with dimensions of about 4.60 x 1.50 x 4.00 mm^3. One surface of each sample was polished using 1200 , 4000 grit sizes of SiC grinding paper. A short notch of about 0.5 mm of length was cut on the 4.60 mm x 4.00 mm surface of samples and a pre-crack initiated on the polished surface was at the end of the notch using a 1 kg Vickers indent. To eliminate the residual stress around the crack due to indentation, the samples were annealed at 600 ^oC for 5 hours. After annealing, the crack length on the polished surface of each sample was measured. An electrode was coated on the 4.60 x 1.50 mm^2 faces as described previously. The samples were mounted into a fixture under a clamped condition (i.e. the samples were fixed with a screw connected between the electrode surfaces and the power supply). The samples were then submerged in a silicon oil bath and then subjected to a bipolar triangular electrical field of amplitude

± 5.5 kV ($\pm 1.4E_c$) which was applied perpendicular to the crack surface up to 10^4 cycles. In this experiment, the samples were tested with three different frequencies: 10 Hz, 50 Hz and 100 Hz. After fatigue testing, the spatial distribution of domain orientations around the crack tip was investigated using synchrotron x-ray diffraction. The experimental setup for x-ray measurement is shown in Fig. 1. In this investigation, a high spatial resolution and high energy x-ray beam was obtained from a synchrotron source at beamline ID15B at the European Synchrotron Radiation Facility (ESRF). To obtain the maximum penetration of the PZT samples and to avoid background scatter, the average energy of the x-ray was selected at 87.62 keV which is just below the energy to excite the background due to the Lead K-edge (88 keV) fluorescence x-ray. The beam size was set to 150 μm x 150 μm by a set of tungsten slits just prior to the sample. An area of 3.50 x 2.50 mm^2 around the crack tip was scanned by translating the sample through the beam. Diffraction patterns in the form of Debye-Scherrer rings were collected using an x-ray image intensifier coupled with a FReLoN CCD camera. The two dimensional images (Debye-Scherrer rings) were "caked" (sectioned into 24 parts with the azimuth angle or eta angle, η of 15^o increments) into one dimensional diffraction patterns using the radial integration software fit2d (Hammersley, Svensson et al. 1994). The complete distribution of in-plane orientated domain orientation may be presented by the 002/200 intensity ratio obtained from different scattering vectors parallel to eta angles, η. The integrated intensity was calculated from curve fitting using a split Pearson VII profile shape function with Matlab (Ver. 7.0) and used to estimate the domain fractions [(Daniels, Jones et al. 2006)].

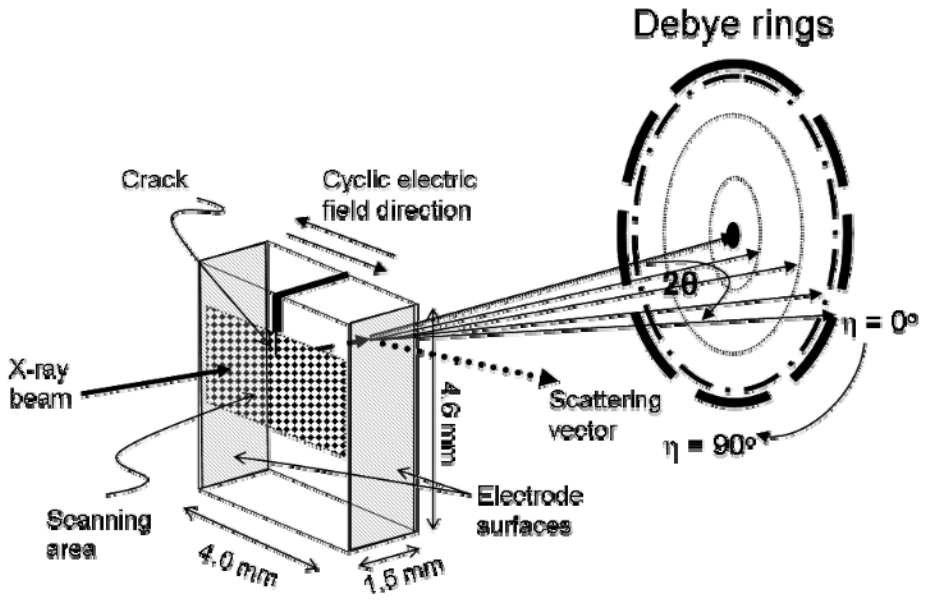

Fig. 1. Experimental setup for investigating domain orientation distribution around a crack tip by using high-energy x-ray diffraction.

Results

Domain switching behaviour of pre-cracked samples

After the pre-cracked samples were subjected to the cyclic electrical loading at frequencies of 10 Hz, 50 Hz, and 100 Hz, the optical micrographs of crack propagation of each sample were recorded and are shown in Fig. 2a, 2b, and 2c for 10 Hz, 50 Hz, and 100 Hz, respectively. The approximate crack length of each sample before and after being subjected to the cyclic loading is measured and shown in Table 1. These results show that electrically induced crack propagation rate is much more pronounced if a sample is fatigued with a lower frequency. The crack length after 10^4 fatigue cycles is about 125 μm (increases by about 38%) after cycling at 10 Hz, 50 μm (increases by about

10%) at 10 Hz, and 25 μm (increases by about 4%) at 100 Hz for the sample subjected to a cyclic loading at 10 Hz, 50 Hz and 100 Hz respectively.

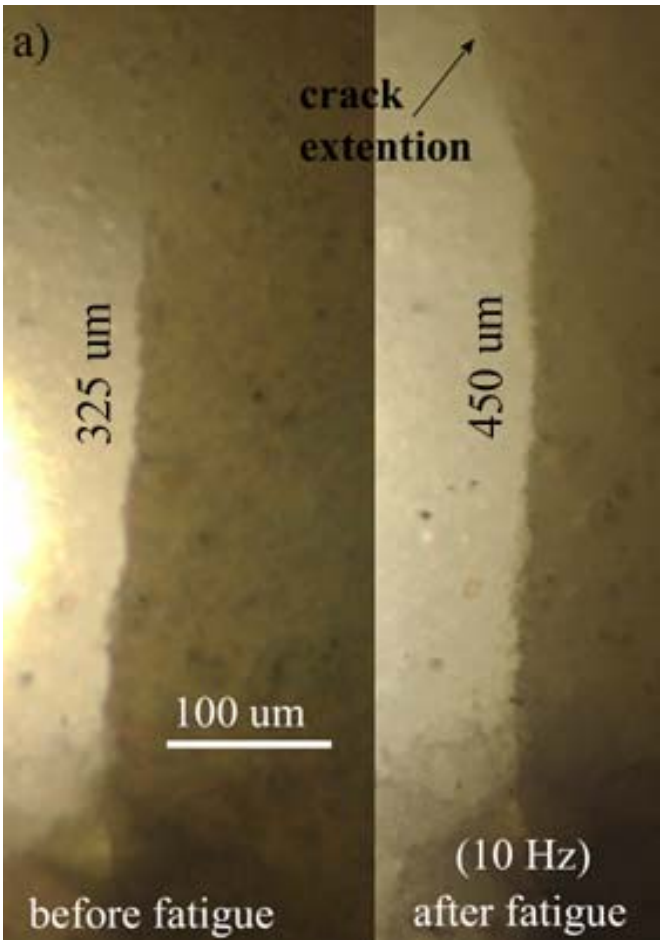

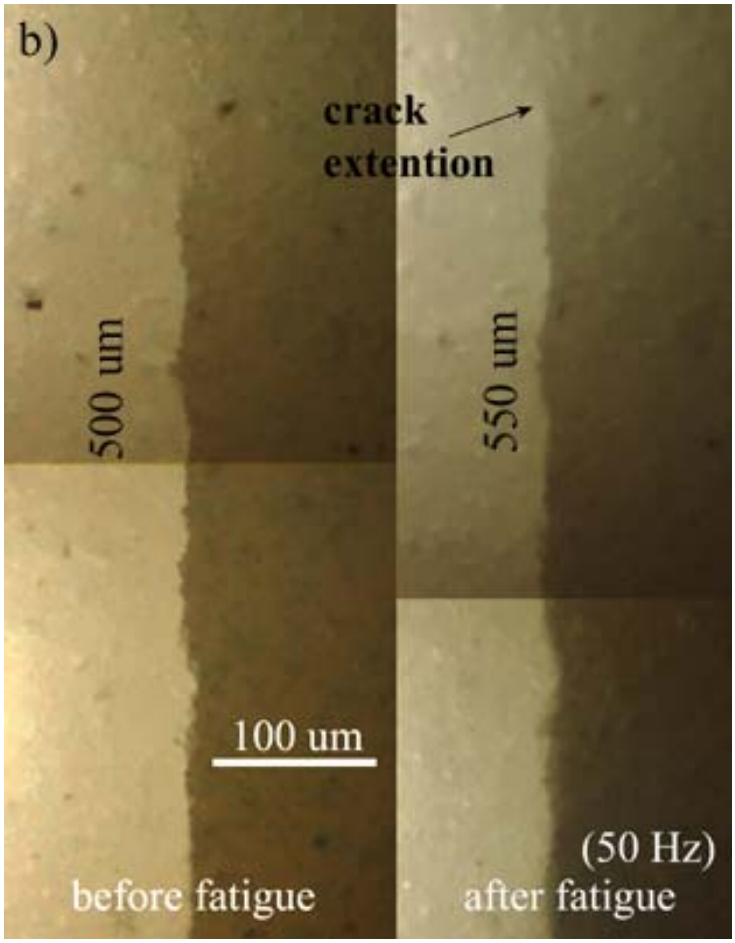
b)
crack
extention
500 um
550 um
100 um
(50 Hz)
before fatigue
after fatigue

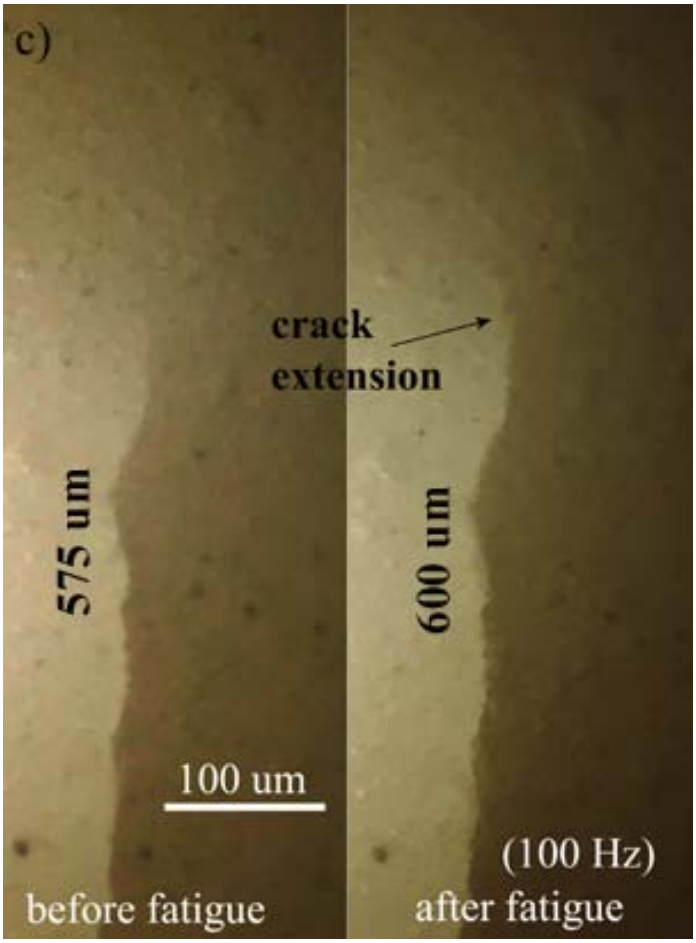

Fig. 2. The optical micrographs of samples before and after fatigue testing at (a) 10 Hz, (b) 50 Hz, and (c) 100 Hz of a bipolar electric field.

Table.1. The approximate crack length of the fatigued samples under ±1.4 kV/mm of bipolar cyclic loading with different frequencies.

Sample	Frequency (Hz)	Initial crack length, a_i (μm)	Crack length after 10^4 cycles of fatigue, a_f (μm)	Crack growth length, Δa	
				μm	%
A	10	325	450	125	38
B	50	500	550	50	10
C	100	575	600	25	4

In this experiment, besides the effect of frequency, the different stress intensities due to the changing crack length may have an influence on crack propagation. Under the electrical loading, strain induced by domain switching occurs around the crack tip. As the result of domain switching strain, a stress concentration is generated around the crack tip [(Yang and Suo 1994)]. In this case, the crack propagates when the electric field intensity of the crack tip is high enough to induce the critical stress intensity factor (K_{IC}). To consider the effect of the crack length as well as the relationship between the electric field intensity and stress intensity factor, the formulae provided by Yang and Suo [(Yang and Suo 1994)] are applied as follows:

$$K_E = \frac{E}{h}\sqrt{2h \tan(\pi a_i/2h)} \quad (1)$$

where K_E is the intensity of the crack tip electrical field, h is the distance between electrode surfaces, E is the amplitude of the applied electric field, and a_i is the initial crack length,

$$K_I = \beta \frac{Y\gamma_s}{E_c} K_E \quad (2)$$

where K_I is the stress intensity factor, Y is Young's modulus, γ_s is electrostrictive strain, E_c is the coercive field, and β is a dimensionless parameter depending on the crack condition (i.e. $\beta \sim 0.25$ for an insulating crack).

By substituting equation 1 into equation 2, the relationship between stress intensity factor and the electric field can be expressed as:

$$K_I = \beta \frac{Y \gamma_s}{E_c} \frac{E}{h} \sqrt{2h \tan(\pi a_i / 2h)}. \qquad (3)$$

Considering equation 3, the stress intensity, K_I, is higher if the initial crack length, a_i, is longer. Consequently, the greatest crack propagation, Δa, in Table 1 should be observed in the sample possessing the longest initial crack length, a_i, (i.e. sample C). However, the results from this experiment show that the sample with the longest initial crack length (sample C) exhibits the shortest crack propagation while the sample with the shortest initial crack length (sample A) possesses the longest or most severe crack propagation. This implies that the effect of cyclic frequency dominates crack propagation under cyclic electric loading. Furthermore, these results show that although the samples were subjected to the same amplitude of cyclic field, the most severe crack propagation occurs under the lowest cyclic frequency of the field. This finding is outlined in Table 2.

Table 2 compares the different situations between crack propagation dominated by the effect of stress intensity (*case 1*) and frequency (*case 2*). The experimental results agree with case 2 which supports the frequency effect phenomenon. $\Delta a(A')$, $\Delta a(B')$, $\Delta a(C')$ denote crack propagation under 10 Hz, 50 Hz, and 100 Hz in *case 1* respectively; and $\Delta a(A)$, $\Delta a(B)$, $\Delta a(C)$ in *case 2*.

Independent input parameters						Crack propagation, Δa (μm)			
Initial crack length, a_i (μm)		Stress intensity equation 3		Frequency (Hz)		*Case 1*: Effect of stress intensity (equation 3)		*Case 2*: Effect of frequency (experimental results)	
a_i (A) = 325	⇐ increase	K_I (A)	increase, ⇐ a_i (C) > a_i (B) > a_i (A)	10	⇐ increase	$\Delta a(A')$	increase, ⇐ $\Delta a(C') > \Delta a(B') > \Delta a(A')$	$\Delta a(A)$ =125	decrease, ⇐ $\Delta a(C) < \Delta a(B) < \Delta a(A)$
a_i (B) = 500		K_I (B)		50		$\Delta a(B')$		$\Delta a(B)$ = 50	
a_i (C) = 575		K_I (C)		100		$\Delta a(C')$		$\Delta a(C)$ = 25	

Considering the results from bulk samples and fracture samples, a relationship can be seen between frequency, polarization and crack propagation. At the lower frequency, the polarization decays faster and crack propagation per cycle is greater compared with the case of higher frequency. These relationships may be attributed to domain switching behavior which is the driving force of polarization degradation and crack propagation under the cyclic loading.

To investigate the micro-mechanism of domain switching around the crack tip under cyclic electric loading, the fatigued pre-cracked samples were investigated by using a high spatial resolution and high energy x-ray beam. Domain switching behavior of the fatigued samples is characterized by the change of the intensities of 002 and 200 peaks representing the c- and a- domains, respectively. The preferred orientations of in-plane domains can be indicated by the integrated intensity ratio of 002 to 200 peaks of which the scattering vector is approximately parallel to the sample surface (see Fig. 1). An example of diffracted intensity of the 002 and 200 peaks as well as fitting curves for the tetragonal phase is shown in Fig. 3.

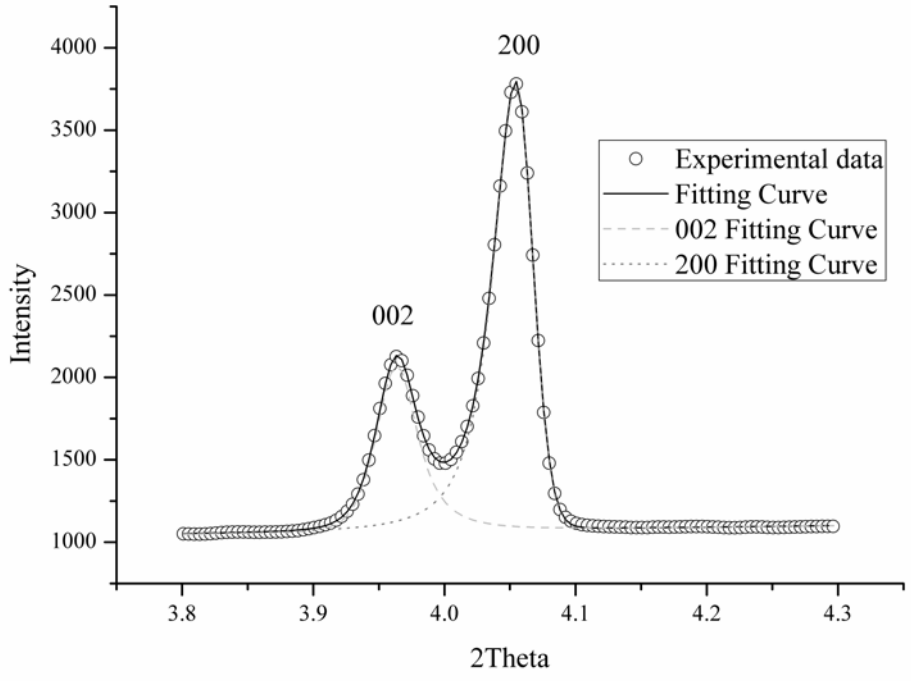

Fig. 3. 002 and 200 peaks and fitting curves using a split Pearson VII profile shape function.

The preferred orientation of c-domain along the electric field direction is indicated by the multiple of a random distribution (MRD) which is expressed by:

$$MRD_{002} = 3\frac{\left(I_{002}/I^{R}_{002}\right)}{\left(I_{002}/I^{R}_{002}\right)+2\times\left(I_{200}/I^{R}_{200}\right)} \quad (4)$$

where I_{002} and I_{200} is the integrated intensity of the 002 and 200 peaks of a fatigued sample which possesses preferred domain orientation [(Jones, Slamovich et al. 2005)]. The superscript R denotes the integrated intensity of the same peaks for a sample with random domain orientation. From equation 4, if the preferred orientation of c-domains is away from the electric field direction, MRD_{002} is approximately 0. If the orientation of the domains is random, $MRD_{002} = 1$ and if there is preferred orientation along the given direction (i.e. the scattering vector direction), MRD_{002} becomes larger than 1. MRD_{002} values obtained from the scanning area around a crack tip are plotted as a function of position relative to the crack tip and direction in the plane of the sample and are represented as a contour. Domain distribution contours of samples fatigued at 10 Hz, 50 Hz, and 100 Hz are presented in Fig 4, 5 and 6, respectively. For each frequency, a set of four contours is shown representing different directions with respect to the crack face or applied field (or eta angles, η, see Fig. 1). The distributions of domain orientations around the crack tip can be interpreted by the combination of two indicators. The first indicator is the direction of a preferred orientation which is represented by an arrow at the

left top corner of each contour plot. The second one is the MRD_{002} values calculated using equation 4. For example, in Fig. 4, the preferred c-domain zone (i.e. $MRD_{002} > 1$) which orients parallel to the applied field, $\eta = 0^o$ (or perpendicular to the crack face), can be revealed by contour a1 and these oriented $\eta = 45^o$, 90^o, and 135^o to the applied field are represented by contours a2, a3, and a4, respectively. Moreover, the complete texture of in-plane domains can be obtained by the combination of contours of all η from 0^o to 180^o. However, for simplicity, the contours in these figures are taken from just four selected angles ($\eta = 0^o$, 45^o, 90^o, and 135^o). For example, in Fig. 4, contour a1 ($\eta = 0^o$) reveals the preference for c-domain orientations parallel to the applied electric field direction (perpendicular to the crack face). Also, contour a2 ($\eta = 45^o$), a3 ($\eta = 90^o$), and a4 ($\eta = 135^o$) describes the preferred c-domain orientations at 45^o, 90^o, and 135^o to the electric field.

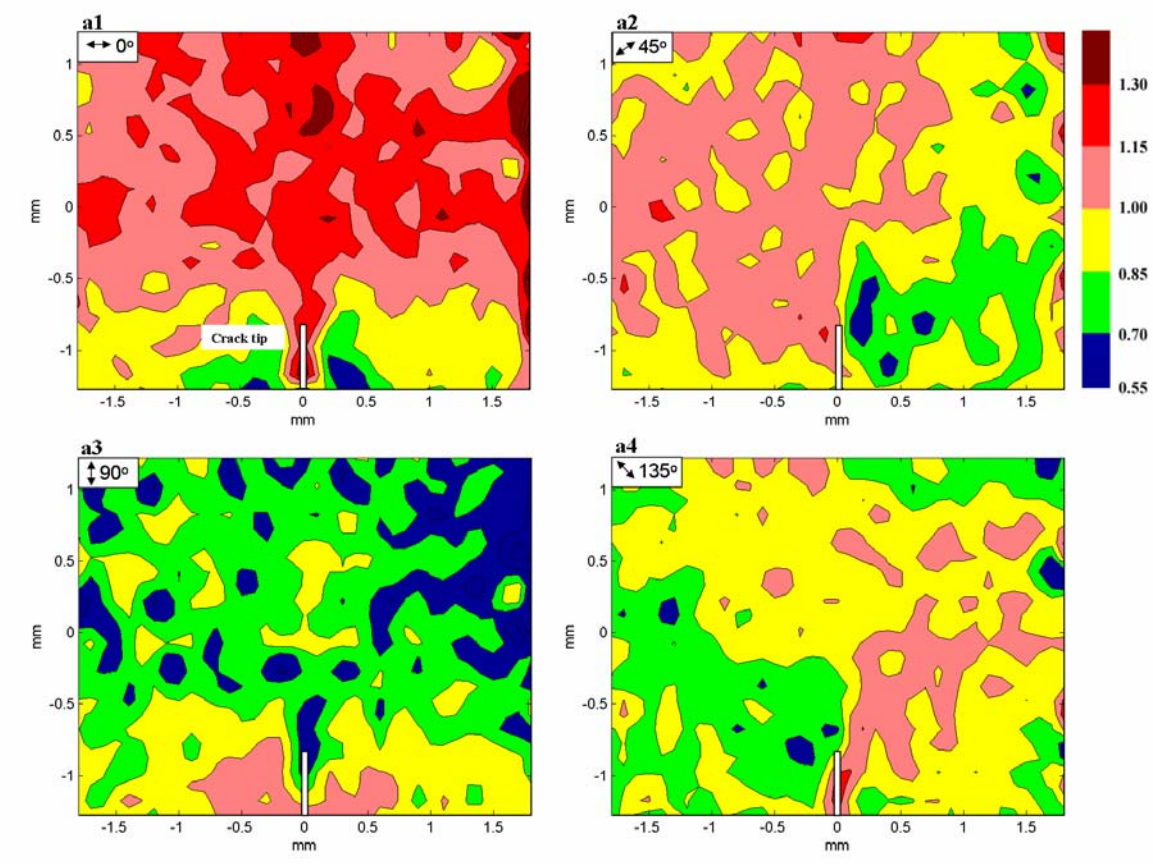

Fig. 4. Domain contours around the crack tip in a fatigued sample (sample A) after 10^4 cycles under a frequency of 10 Hz at different preferred orientations of c-domain. The direction with respect to η of the c-domains is represented by the arrow at the top left corner of each contour. The MRD_{002} values are indicated by a color bar next to the contour.

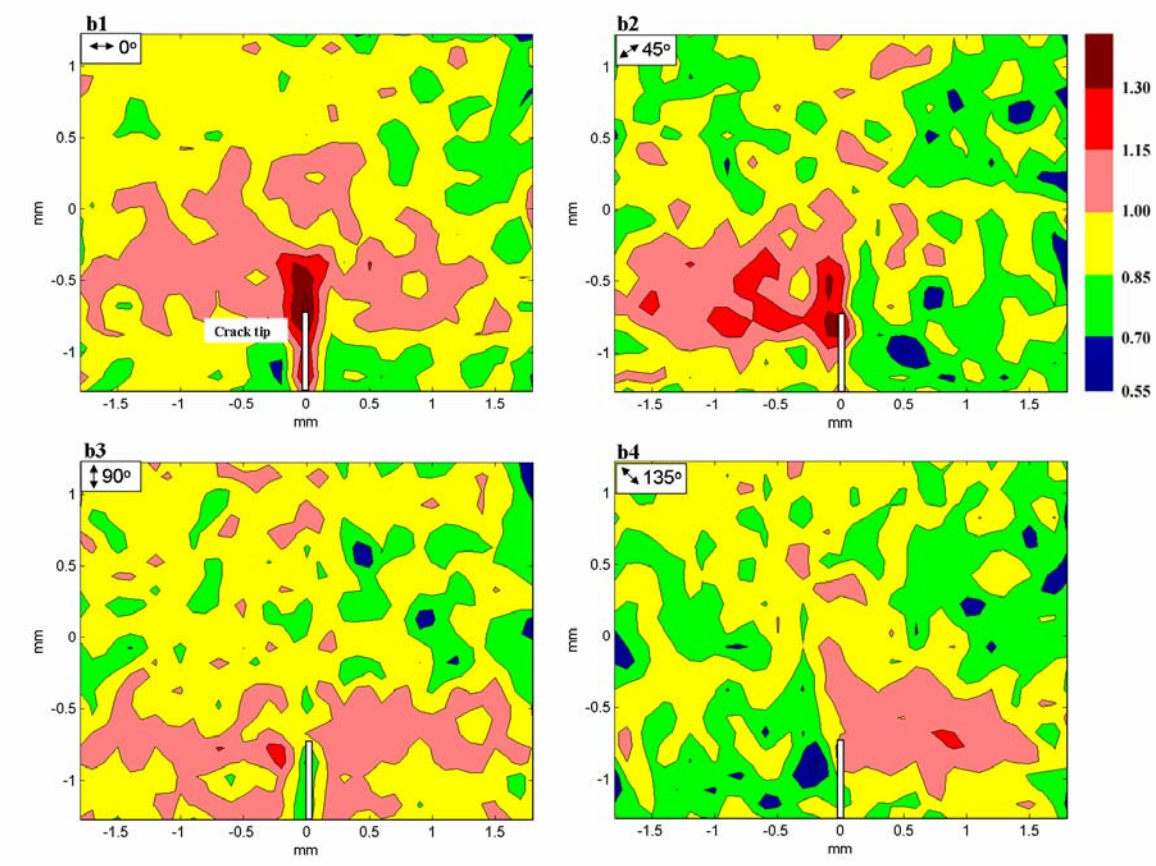

Fig. 5. Domain contours of a fatigue sample (sample B) after 10^4 cycles at a frequency of 50 Hz at different η angles with respect to the applied field: 0^o, 45^o, 90^o, 135^o.

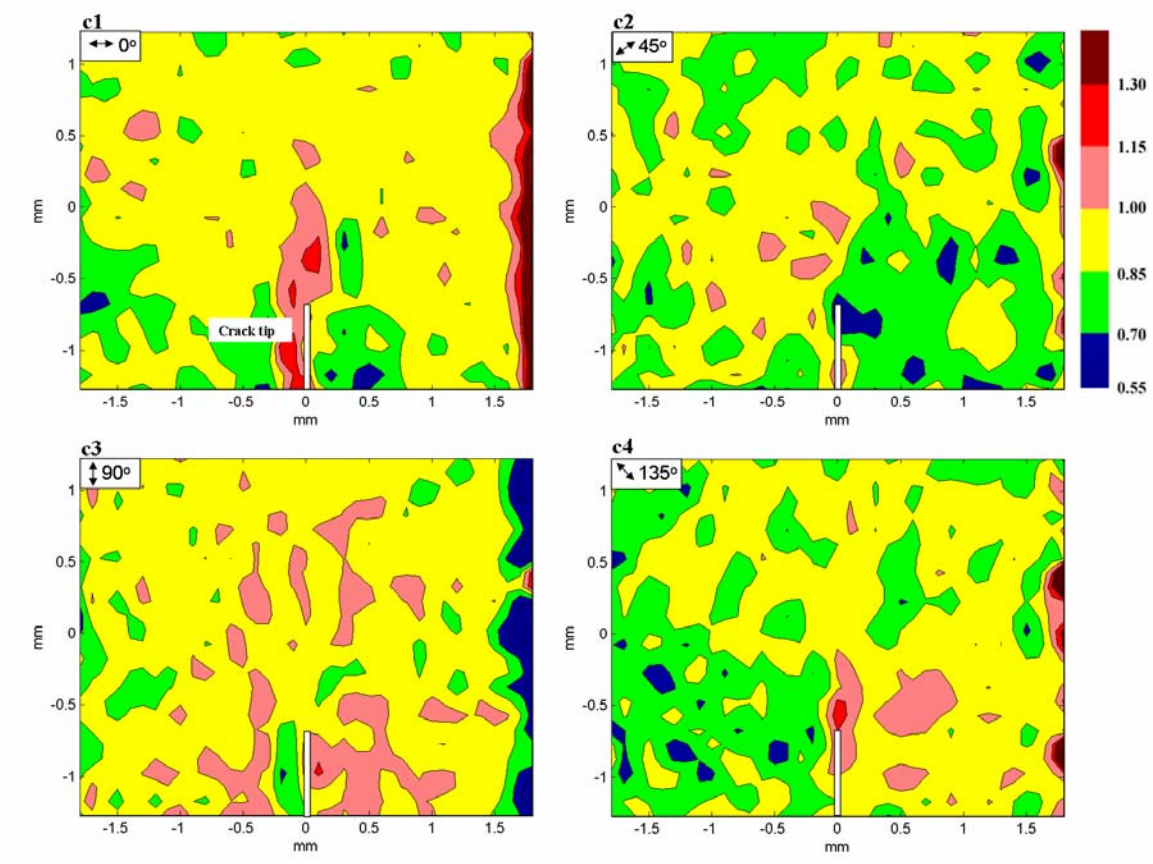

Fig. 6. Domain contours of a fatigue sample (sample C) after 10^4 cycles at a frequency of 100 Hz at different η angles with respect to the applied field: 0^o, 45^o, 90^o, 135^o.

The right hand side of each plot shows an abnormally high level of MRD_{002} in each sample. This is related to the interface between the ceramics and electrode, which leads to the very strong preference of the in-plane c-domains in that area. The data can be ignored for this analysis as they are well removed from the crack tip. For Fig. 4 to 6, the contours of the $\eta = 0^o$ and 90^o show symmetry of domain orientation distributions about the crack face while those of the $\eta = 45^o$ and 135^o are asymmetric. The preferred orientations about the crack tip of each fatigued sample can be observed when considering the four η angles together. By comparing the area of preferred c-domain

orientations of sample A, B, and C in Fig. 4, 5, and 6 respectively, it can be seen that they differ with varying frequency. After being fatigued under low frequency (10 Hz), the zone of preferred c-domain orientations, which represents by $MRD_{002} > 1$, is considerably larger than that of the 50 and 100 Hz samples. This may imply that after being fatigued at 10^4 cycles, the frequency effect could be investigated by the size of preferred c-domain orientation zone which reflects the irreversible domain switching. The degree of irreversible domain switching under lower frequency (10 Hz) loading is higher than that of higher frequency (50 Hz, and 100 Hz). This leads to a reduction of the mobility of 90^o domain walls during cyclic loading which may be attributed to domain wall pinning by defects [(Shvartsman, Kholkin et al. 2005), (Nuffer, Lupascu et al. 2000), (Tagantsev, Stolichnov et al. 2001), (Scott and Dawber 2000)]. Consequently, the polarization fatigue takes place (i.e. the remnant polarization decreases with the increase of cycle number. Besides polarization fatigue, the results obtained from domain contours can be used to investigate the relationship between the domain switching behavior and crack propagation. Considering domain contours of each fatigued sample, the non-uniform domain orientation distributions can be observed. The preferred c-domains oriented 0^o, 45^o and 135^o to the field (or 90^o, 135^o, and 45^o to the crack face) takes place in front of the crack tip while those oriented 90^o to the field occurs at the crack flanks and behind the crack tip. These results agree with the model presented by T. Zhu [(Zhu, Fang et al. 1999)] and H.G. Beom [(Beom and Jeong 2005)]. Moreover, it can be observed that the switching zone of preferred c-domains orientated at 45^o and 135^o to the crack face is smaller and exhibits a weaker degree of preferences than those orientated 90^o to the crack face. To simplify this explanation, the distributions of preferred c-domain orientations

are schematically shown in Fig 7. In this experiment, the non-uniform distributions of preferred c-domain orientations around the crack tip may be attributed to the inhomogeneous local field around the crack (see Fig. 7b). The inhomogeneous field is caused by the crack conditions (i.e. crack geometry, impermeable, or permeable boundary conditions of the crack faces) within the samples. Since the samples were submerged in a silicon bath while being electrically fatigued, it can be expected that the silicon oil film may fill a gap between crack surfaces. Therefore, it can be assumed that a crack becomes insulating (if the oil fully fills the gap and there is no free space between the crack faces) or semi-insulating (if the oil partially fills the gap and there is free space between the crack faces). Being shielded by the crack fully or partially filled with the oil, the electric flux lines deflect around the crack tip and concentrate at the crack tip [(Suo 1993), (Wang and Singh 1997), (Zhu and Yang 1997), (Fang, Yang et al. 2005),(Westram, Oates et al. 2007)]. Consequently, this inhomogeneous field causes the non-uniform distribution of preferred domain orientations (i.e. preferred c-domain oriented 0^o to the crack face occurs at the crack face behind the crack tip while that oriented 90^o, 45^o or 135^o to the crack face takes place at the front of the crack tip). This leads to large strain mismatch, which is the driving force for crack propagation [(Westram, Oates et al. 2007)], between the area in front of the crack tip and behind the crack tip. Under cyclic electrical loading, when the field increases above the coercive field, 90^o domain switching occurs and non-uniform domain orientation distribution is induced by the inhomogeneous local field around the crack. Consequently, strain mismatch around the crack tip is larger which results in the increase of a stress intensity.

If the stress intensity reaches the critical value (K_{Ic}) of the ceramics, crack starts propagating.

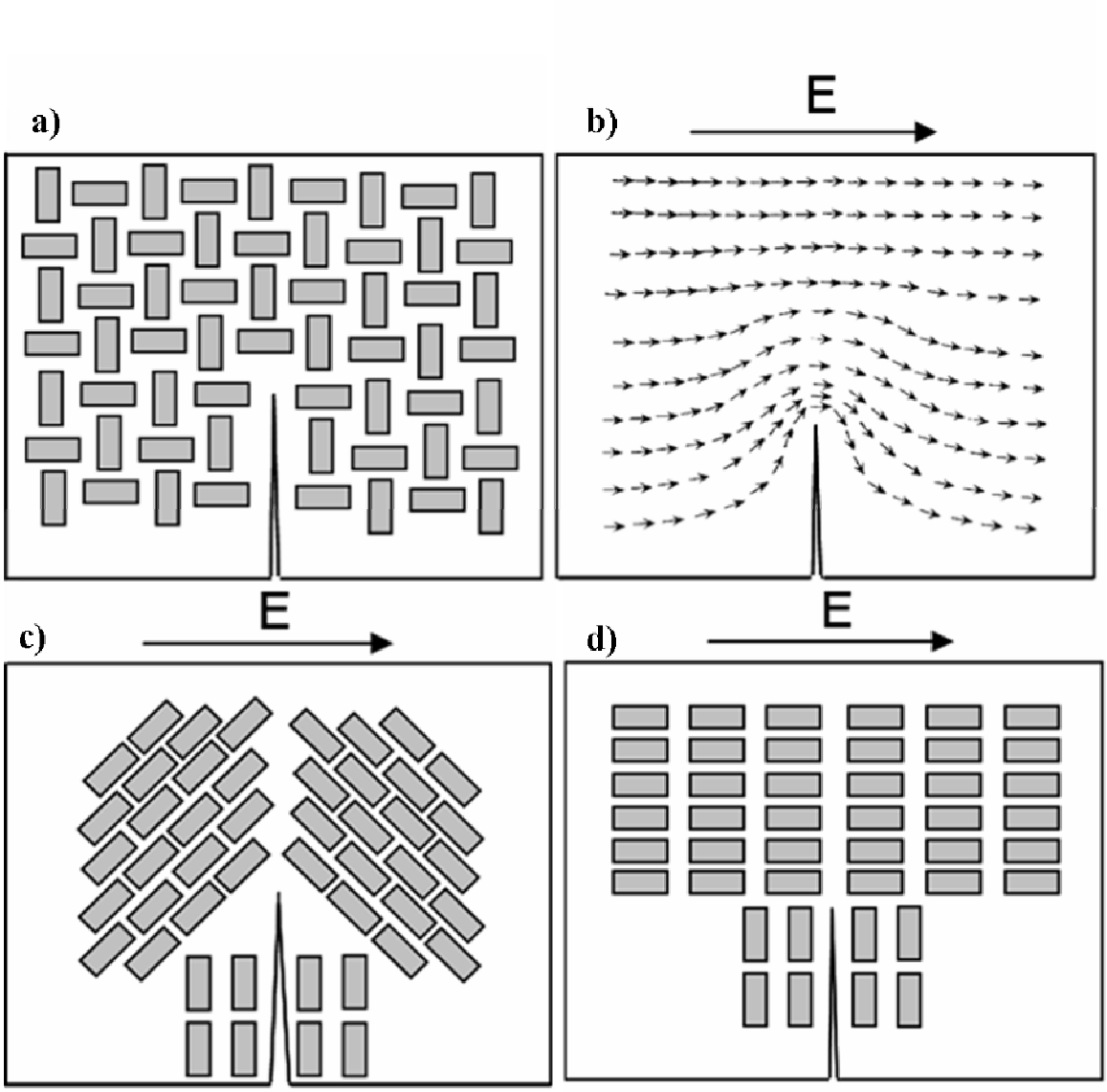

Fig. 7. A schematic diagram showing the relationship between the domain orientations and the local field around the crack: (a) represents the random orientations before being fatigued; (b) the local field; (c) a preferred c-domain oriented 45^o, 135^o and 90^o to the crack face after fatigue; (d) A preferred c-domain oriented 0^o and 90^o to the crack face after fatigue. The driving force for crack propagation is the large strain mismatch induced

by the non-uniformity of preferred c-domain orientations ahead and behind the crack tip caused by the inhomogeneous field.

Model of the frequency effect on crack propagation

Besides the influence of an inhomogeneous electric field and non-uniform domain orientation distributions around a crack tip, the frequency of an applied field also affects the severity of crack propagation. To logically explain the micro-mechanism of crack growth due to domain switching under different frequencies of an electric field, a model presented by the author in the previous work [(Pojprapai (Imlao), Jones et al. 2008)] explaining bulk PZT fatigue, is modified and used to explain the frequency effect on crack growth. This model describes the frequency-dependent domain behavior and mechanical fatigue effect using a viscoelasticity-based concept. This viscoelasticity-based model presented that the ferroelastic strain induced by 90^{o} domain wall movement of bulk ceramics can be expressed by

$$\varepsilon(t) = Ae^{-t/\theta} + C' \tag{5}$$

where $\varepsilon(t)$ is ferroelastic strain as a function of time, θ is relaxation time, as well as A and C' are constants. This model and the experimental result of the previous work shows that the relaxation time of domain movement at lower frequency fatigue (1 Hz) is longer than that at higher frequency fatigue (20 Hz); the ferroelastic strain at lower frequency is, also, larger than that at higher frequency.

In the case of crack propagation under different frequencies of electric loading, the same viscoelasticity-based concept may be used to explain the link between the frequency of the applied field, domain switching behaviour, and crack propagation. To unravel this

complicated relationship, the domain switching process around the crack tip under different loading frequencies is shown schematically in Fig. 8.

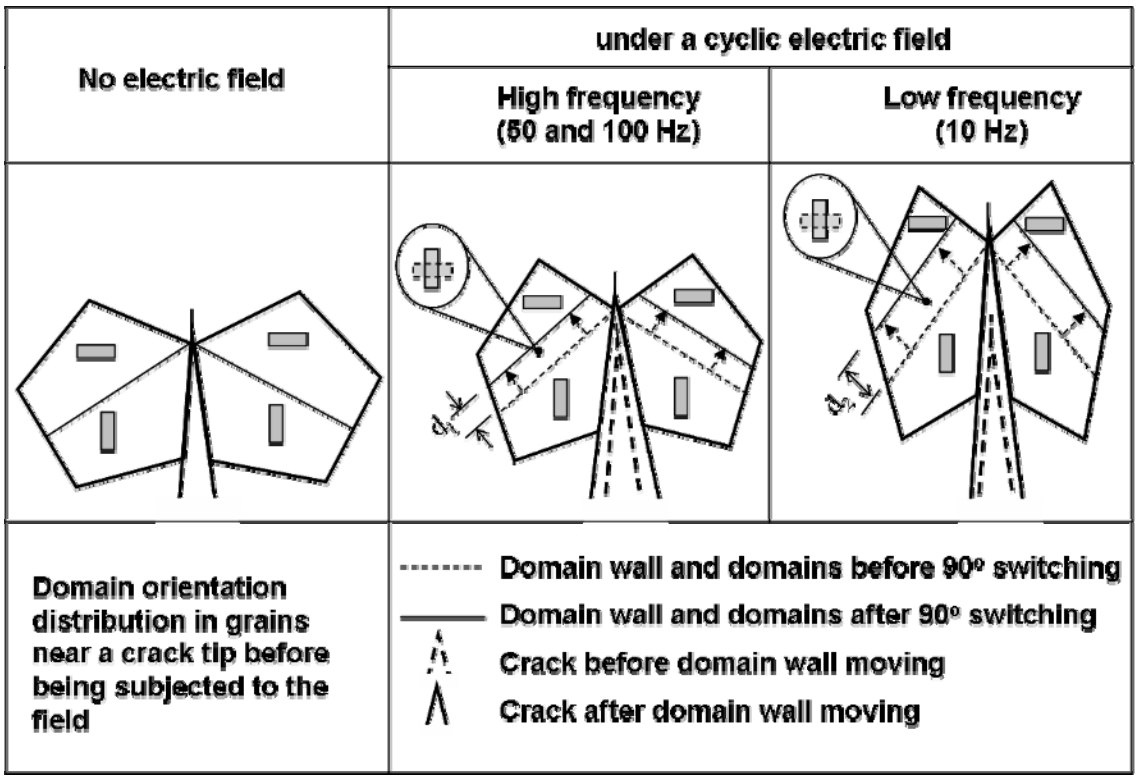

Fig. 8. The schematic diagram presents the effect of frequency on domain wall movement near the crack tip. Domain walls are able to travel over longer distance ($d_2 > d_1$) under a lower frequency which leads to high local deformation and more severe crack growth compared with a higher frequency.

From Fig. 8, under a cyclic loading, when the electrical load increases, domain walls move over a certain distance due to a local electric field. When the load decreases during a cycle, some domain walls move back while some domain walls do not revert to the original position because they may be pinned by defects within the grains [(Shvartsman, Kholkin et al. 2005), (Nuffer, Lupascu et al. 2000), (Tagantsev, Stolichnov et al. 2001)]. At the switching zone just behind the crack tip, these pinned domain walls, therefore,

may cause high local strain and initiate crack opening. In the case of low frequency, domains at the switching zone behind the crack tip experience a longer time under the local field for a single cycle; as a result, domain walls are able to travel over a longer distance due to viscoelastic effects described in Fig. 8. Therefore, a higher local strain is induced at such switching zone and wedges the crack open, hence more severe crack propagation. On the other hand, if the higher frequency of an electric field is applied, domain walls move over a shorter distance compared with the first case. Consequently, the lower local deformation, which takes place at the switching zone just behind the crack tip, may cause less crack propagation per cycle compared with the case of a low frequency-loading.

Conclusion

Experimental results showed that a greater rate of crack propagation with decreasing frequency. Spatial analysis of c-domain orientations around a crack tip showed that a clear zone of preferred domain orientations. The orientation of the c-domains can be predicted using the path of the electric field around an insulating crack. Additionally, the size of the zone of preferred domain orientations increased with decreasing frequency.

It is therefore concluded that:

1. Cyclic fatigue crack growth in piezoelectric materials is caused by strain mismatch at the crack tip caused by domain re-orientations induced by the path of the electric field.
2. The magnitude of this mismatch decreases with increasing frequency due to reduced amount of domain re-orientation per cycle owing to the viscoelastic nature of the domain

movement.

3. Hence, fatigue crack growth rates per cycle decrease with increasing cycling frequency.

References

Beom, H. G. and K. M. Jeong (2005). "Crack growth in ferroelectric ceramics under electric loading." Acta Mechanica **177**(1): 43-60.

Daniels, J. E., J. L. Jones, et al. (2006). "Characterization of domain structures from diffraction profiles in tetragonal ferroelastic ceramics." Journal of Physics D: Applied Physics **39**(24): 5294-5299.

Fang, D., B. Liu, et al. (2004). "Fatigue crack growth in ferroelectric ceramics driven by alternating electric fields." Journal of the American Ceramic Society **87**(5): 840-846.

Fang, F., W. Yang, et al. (2005). "FATIGUE CRACK GROWTH FOR BaTiO 3 FERROELECTRIC SINGLE CRYSTALS UNDER CYCLIC ELECTRIC LOADING." Journal of the American Ceramic Society **88**(9): 2491-2497.

Hall, D. A., A. Steuwer, et al. (2006). "Analysis of elastic strain and crystallographic texture in poled rhombohedral PZT ceramics." Acta Materialia **54**(11): 3075-3083.

Hammersley, A. P., S. O. Svensson, et al. (1994). "Calibration and correction of spatial distortions in 2D detector systems." Nuclear Instruments and Methods in Physics Research Section A: Accelerators, Spectrometers, Detectors and Associated Equipment **346**(1-2): 312-321.

Jones, J. L., M. Hoffman, et al. (2007). "Ferroelastic domain switching in lead zirconate titanate measured by in situ neutron diffraction." Mechanics of Materials **39**(4): 283-290.

Jones, J. L., S. M. Motahari, et al. (2007). "Crack tip process zone domain switching in a soft lead zirconate titanate ceramic." Acta Materialia **55**(16): 5538-5548.

Jones, J. L., E. B. Slamovich, et al. (2005). "Domain texture distributions in tetragonal lead zirconate titanate by x-ray and neutron diffraction." Journal of Applied Physics **97**: 034113.

Kungl, H. and M. J. Hoffmann (2007). "Temperature dependence of poling strain and strain under high electric fields in LaSr-doped morphotropic PZT and its relation to changes in structural characteristics." Acta Materialia **55**(17): 5780-5791.

Lente, M. H. and J. A. Eiras (2001). "90° domain reorientation and domain wall rearrangement in lead zirconate titanate ceramics characterized by transient current and hysteresis loop measurements." Journal of Applied Physics **89**: 5093.

Lente, M. H. and J. A. Eiras (2001). "Frequency dependence of the switching polarisation in PZT ceramics." Ferroelectrics **257**(1): 227-232.

Lupascu, D. C. (2004). Fatigue in Ferroelectric Ceramics and Related Issues, Springer.

Nuffer, J., D. C. Lupascu, et al. (2000). "Damage evolution in ferroelectric PZT induced by bipolar electric cycling." Acta Materialia **48**(14): 3783-3794.

Picinin, A., M. H. Lente, et al. (2004). "Theoretical and experimental investigations of polarization switching in ferroelectric materials." Physical Review B **69**(6): 64117.

Pojprapai (Imlao), S., L. J. Jones, et al. (2008). "Ferroelastic domain switching fatigue in lead zirconate titanate ceramics." Acta Materialia.

Pojprapai, S., J. L. Jones, et al. (2006). "Domain Switching Under Cyclic Mechanical Loading in Lead Zirconate Titanate." Journal of the American Ceramic Society.

Pojprapai, S., J. L. Jones, et al. (2008). "Ferroelastic domain switching fatigue in lead zirconate titanate ceramics." Acta Materialia.

Scott, J. F. and M. Dawber (2000). "Oxygen-vacancy ordering as a fatigue mechanism in perovskite ferroelectrics." Applied Physics Letters **76**: 3801.

Shvartsman, V. V., A. L. Kholkin, et al. (2005). "Investigation of fatigue mechanism in ferroelectric ceramic via piezoresponse force microscopy." Journal of the European Ceramic Society **25**(12): 2559-2561.

Suo, Z. (1993). "Models for breakdown-resistant dielectric and ferroelectric ceramics." Journal of the Mechanics and Physics of Solids **41**(7): 1155-76.

Tagantsev, A. K., I. Stolichnov, et al. (2001). "Polarization fatigue in ferroelectric films: Basic experimental findings, phenomenological scenarios, and microscopic features." Journal of Applied Physics **90**: 1387.

Wang, H. and R. N. Singh (1997). "Crack propagation in piezoelectric ceramics: Effects of applied electric fields." Journal of Applied Physics **81**: 7471.

Westram, I., W. S. Oates, et al. (2007). "Mechanism of electric fatigue crack growth in lead zirconate titanate." Acta Materialia **55**(1): 301-312.

Yang, W. (2002). Mechatronic Reliability: Electric Failures, Mechanical-Electrical Coupling, Domain Switching, Mass-Flow Instabilities, Springer.

Yang, W. and Z. Suo (1994). "Cracking in ceramic actuators caused by electrostriction." Journal of the mechanics and physics of solids **42**(4): 649-663.

Zhu, T., F. Fang, et al. (1999). "Fatigue crack growth in ferroelectric ceramics below the coercive field." Journal of Materials Science Letters **18**(13): 1025-1027.

Zhu, T. and W. Yang (1997). "Toughness variation of ferroelectrics by polarization switch under non-uniform electric field." Acta Materialia **45**(11): 4695-4702.

Zhu, T. and W. Yang (1999). "Fatigue crack growth in ferroelectrics driven by cyclic electric loading." Journal of the mechanics and physics of solids **47**: 81-97.